

# Structural condition monitoring of Coriolis flowmeters through stiffness measurement

Jingqiong Zhang<sup>1</sup>, Tao Wang<sup>2</sup>, Jinyu Liu<sup>1,2</sup>, Yong Yan<sup>1</sup>, Edward Jukes<sup>2</sup>

<sup>1</sup>*School of Engineering and Digital Arts, University of Kent, Canterbury, U.K.*

<sup>2</sup>*KROHNE Ltd, Wellingborough, U.K.*

*E-mail (corresponding author): jz233@kent.ac.uk*

---

## Abstract

Condition monitoring of an abrasive or erosive process is essential to give early warning of potential issues and ensure safe delivery of fluid material via pipeline transportation. As one of the solutions to direct mass flow measurement, Coriolis flowmeters provide highly accurate and repeatable measurements in single phase flow processes. In some multiphase flow processes containing solid particles, Coriolis flowmeters may not perform well or even fail due to erosive wear of the measuring tubes. This paper presents an in-situ technique to monitor the structural conditions of a Coriolis flowmeter by analyzing a stiffness related diagnostic parameter in order to validate measurements or prevent flowmeter failure.

This paper demonstrates the procedure to extract the stiffness related diagnostic parameter from a Coriolis flowmeter, on the basis of a mathematical model of the Coriolis oscillation system. With the aid of additional frequencies applied to the drive signal, the stiffness related diagnostic parameter of the measuring tubes is determined through frequency response analysis. This stiffness diagnostic parameter is linked to the physical stiffness of the measuring tubes by introducing a scaling factor. Furthermore, various vibration models, with different degrees of freedom and damping levels, are used to simulate the stiffness diagnostics in Coriolis flowmeters. The feasibility and repeatability of the proposed method are verified through computer simulation and experimental tests. The results show that the proposed method performs well in determining the stiffness related diagnostic parameter of a Coriolis flowmeter and hence the verification of its structural condition.

---

## 1. Introduction

Erosive wear results in severe problems in a wide range of processes, particularly in the oil, gas, mineral and metal mining industries. The solid particles in a transportation pipeline system may collide with the piping components such as pipe sections, pipe fittings, valves, flanges, flowmeters and other measurement devices. Consequently, wear problems will affect the operation, performance and service lifespan of such equipment and sometimes even lead to a failure of the whole piping system. It is therefore essential to develop techniques for the condition monitoring of abrasive and erosive processes such as slurry flows where wear problems may occur.

There has been considerable research in developing techniques for condition monitoring of slurry flow processes [1]. El-Alej et al. [2] demonstrated an active acoustic method to monitor sand transportation in sand-water flow. An electrical resistance tomography method, which can visualize the distribution of the sand phase, has been proposed by Faraj et al. [3]. Gao et al. [4] designed an ultrasonic sensing system to investigate the

interactions between sand particles and the pipe wall. However, the main effort of the previous work is devoted to measure and characterize sand particles in order to ensure smooth slurry transportation.

There have been some studies to examine the structural conditions of piping components such as a flowmeter. Through a series of erosive tests on three different types of flowmeters, measurement errors arising from wear problems, were reported in [5]. The performances of two Coriolis flowmeters from two different manufacturers along with a turbine meter and a venturi meter were compared through experimental tests. Some structural information, available from the diagnostic function of one Coriolis flowmeter's manufacturer, was also recorded and linked to erosive wear on the flowmeter. However, no detailed description of the diagnostic function was given. A photo of the erosion scars on the measuring tubes of a Coriolis flowmeter is shown in Figure 1. Investigations into Coriolis flowmeters of three main manufacturers [6-8] have indicated that they are all able to provide some diagnostic data to examine the structural condition of the flowmeter. Some manufacturers have already released this diagnostic

feature into their commercial products [6]. However, limited theoretical research and analytical work has been reported about this diagnostic method.



**Figure 1:** Photo of the eroded tubes of a twin bend-tube Coriolis flow meter [5].

This paper introduces a technique to assess the structural conditions of a Coriolis flowmeter. This method is non-intrusive and cost-effective, making it possible to judge if a flowmeter is eroded and if the measurement results are valid in an erosive environment. This paper firstly illustrates the close link between the stiffness parameter and the calibration of a Coriolis flowmeter, and then explains how to extract the stiffness related diagnostic data from the Coriolis oscillation system. In this paper, we conduct, for the first time, mathematical model based computer simulation to analyze the stiffness extraction process and identify the factors in stiffness determination from the theoretical point of view. The simulation under various sceneries, not only validates the feasibility of this method, but also investigates the influence of modal parameters on the stiffness extraction, such as, the effect of damping level and degrees of freedom. Additionally, experimental tests were conducted to assess the performance of the proposed technique.

## 2. Methodology

### 2.1 Working principle and calibration parameters of Coriolis flowmeters

Coriolis flowmeters provide highly accurate single phase mass flow measurement in a wide variety of liquid and gas applications. A typical Coriolis flowmeter consists of two measuring tubes (twin-tube). Along each measuring tube, a drive coil and magnet pair is positioned at the centre to generate a sinusoidal signal, whilst two electromagnetic sensors are placed at the inlet and outlet of the tube to receive motion signals. When the flow moves through the tube, the two signals are distorted by the Coriolis force, and hence, a time shift,  $\delta_t$ , is created between the signals. The mass flowrate of the flow  $Q_m$  is directly proportional to the time shift [10],

$$Q_m = P_C \delta_t \quad (1)$$

where  $P_C$  is the calibration parameter of the flowmeter, which is determined through a standard calibration process.

Basically, a Coriolis flowmeter continuously tracks the resonant frequency of a fundamental mode,  $f_r$ , which is often referred to as drive or working frequency. Benefiting from this, a Coriolis flowmeter is also capable of providing an independent measurement of the fluid density resulting from the effective vibrating mass,

$$\omega_{r1} = \sqrt{\frac{k_1}{m_1}} \quad (2)$$

Where  $m_1$  denotes the effective vibrating mass, comprising the mass of the empty tube as well as of the fluid in the tube,  $k_1$  represents the stiffness of the measuring tube, and  $\omega_{r1}$  is the angular resonant frequency of the measuring tube vibrating in its fundamental eigenmode.

With an external force ( $F$ ) applied on an object or a structure,  $k_1$  can be defined by the ratio of this force to the resulting displacement ( $\delta x_1$ ) under the same mode,

$$k_1 = \frac{F}{\delta x_1} \quad (3)$$

According to Equations (1) and (2), the constant or unchanged  $P_C$  and  $k_1$  are important for the performance of a Coriolis flowmeter. Over its service life, any changes in the calibration parameters from the original values, obtained from the manufacturer, may result in uncertainties in its specified measurement accuracy and repeatability. However, in an abrasive or corrosive process such as slurry flow, there is a risk that the measuring tubes may be eroded. If erosion occurs, the structural properties of the measuring tubes will change, giving rise to incorrect calibration parameters,  $P_C$  and  $k_1$ , and subsequently errors in the measurements of mass flowrate and density.

Erosion on a Coriolis flowmeter can be observed from the erosion scars on the tube surfaces. Since regular inspections of the internal surfaces of the measuring tubes are impractical to implement, it is desirable develop an online, in-situ monitoring technique to identify erosion. The physical parameter, *stiffness*, of a measuring tube, is a parameter related to its structural condition and also vital for the flowmeter calibration. It is hence of great importance to measure the stiffness of the measuring tube.

### 2.2 Mathematical model of Coriolis flowmeters

According to the working principle of a Coriolis flowmeter, a measuring tube can be modelled using a mass-spring-damper system. Assuming that all the components in the Coriolis oscillation system couple together and follow the same motion, a single measuring tube is simplified by a simplest single degree of freedom (SDOF) model, as shown in Figure 2.

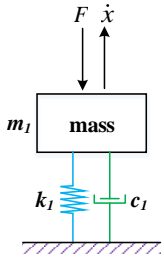


**Figure 2:** SDOF model of a measuring tube of a Coriolis flowmeter.

Here, the effective mass,  $m_1$ , is composed of the effective vibrating mass of a measuring tube and the fluid. The tube acts as the spring, described by the stiffness  $k_1$ . The energy loss, resulting from the interactions between the measuring tube and the environment and other sources, is quantified in terms of the viscous damping coefficient  $c_1$ . The transfer function of the external force and resulting velocity of the lumped mass is given,

$$G_{r1} = \frac{\dot{x}(s)}{F(s)} = \frac{s}{m_1 s^2 + c_1 s + k_1} \quad (4)$$

where  $F$  denotes the force actuated by the drive coil and  $x$  represents the displacement of the lumped mass.

By transferring Equation (4) to the frequency domain, the frequency response function (FRF) of the system is given by,

$$FRF_{phys} = \dot{H}(\omega) = \frac{\dot{x}(\omega)}{F(\omega)} = \frac{j\omega}{-m_1 \omega^2 + j c_1 \omega + k_1} \quad (5)$$

### 2.3 Extraction of stiffness related diagnostic data from frequency response data

Here, we introduce the stiffness related diagnostic parameter to indicate the structural condition of a Coriolis flowmeter. The stiffness related diagnostic parameter is obtained from frequency response of a Coriolis sensing system. In a Coriolis sensing system, the drive signal is proportional to the applied force  $F$ , and the sensor signal is proportional to velocity  $\dot{x}$ . As a result the relationship between the physical FRF data of the measuring tubes and the directly measured FRF data from a Coriolis sensing system can be quantified by a scaling constant,  $A_s$ ,

$$FRF_{meas} = \frac{V_{sensor}}{I_{drive}} = A_s FRF_{phys} \quad (6)$$

By substituting  $FRF_{phys}$  into Equation (6), the measured FRF data from a Coriolis sensing system is written as,

$$FRF_{meas} = \dot{H}_m(\omega) = A_s \dot{H}(\omega) = \frac{j A_s \omega}{-m_1 \omega^2 + j c_1 \omega + k_1} \quad (7)$$

In order to determine the stiffness  $k$ , Equation (7) is split up into the real and imaginary parts,

$$\begin{cases} \text{Re}\{FRF_{meas}(\omega)\} = \text{Re}\{\dot{H}_m(\omega)\} = \frac{A_s c_1 \omega^2}{(k_1 - m_1 \omega^2)^2 + (c_1 \omega)^2} \\ \text{Im}\{FRF_{meas}(\omega)\} = \text{Im}\{\dot{H}_m(\omega)\} = \frac{A_s \omega (k_1 - m_1 \omega^2)}{(k_1 - m_1 \omega^2)^2 + (c_1 \omega)^2} \end{cases} \quad (8)$$

Combining Equations (2) and (8), the stiffness related diagnostic parameter under the flowmeter's fundamental oscillation mode is solved as follows,

$$k_{diag} = \frac{k_1}{A_s} = \frac{\omega_{r1}^2 \omega_{an} \text{Im}\{\dot{H}'(\omega_{an})\}}{(\omega_{r1}^2 - \omega_{an}^2) |\dot{H}'(\omega_{an})|^2} \quad (n = 1, 2, \dots) \quad (9)$$

Where  $\omega_{r1}$  is the angular resonant frequency of the measuring tube vibrating in its first mode and  $\omega_{an}$  represents the additional frequencies, differing from  $\omega_{r1}$ , with the number  $n = 1, 2, \dots$

For the purpose of stiffness measurement, at least one additional frequency,  $f_{a1}$ , is required to apply into the excitation system, apart from the resonant frequency  $f_{r1}$ , according to Equation (9). More additional frequencies yield more stiffness related diagnostic values.

### 2.4 Implementation of stiffness diagnostics

Figure 3 depicts how to implement the stiffness measurement in a Coriolis flowmeter. The drive coil excites the tubes at its resonant frequency, which is determined by the phase control loop. Firstly, one or more additional frequencies are applied to the drive signal on purpose. Secondly, the vibration responses of the measuring tubes, which are induced by these additional frequencies, are collected from the sensor signals [13]. Then, based on quadrature demodulation, the original sensor signal is decomposed into several individual components in terms of frequencies. Next, those separated components in sensor signal corresponding to additional frequency  $f_a$ , are picked out to acquire FRF data,  $FRF_{meas}$ , based on Equation (6). Finally, the stiffness diagnostic value  $k_{diag}$  of the measuring tube is calculated from Equation (9). With reference to the factory baseline data from the manufacturer, the change in stiffness,  $\Delta k_p$ , is determined [6],

$$\Delta k_p = \frac{\Delta k}{k_0} = \frac{k_{diag-situ} - k_0}{k_0} 100\% \quad (10)$$

Where  $k_{diag-situ}$  is the stiffness related diagnostic result during the diagnosis performed by customer in situ, and  $k_0$  denotes the original factory baseline data, which is recorded during the calibration of the flowmeters under factory conditions.

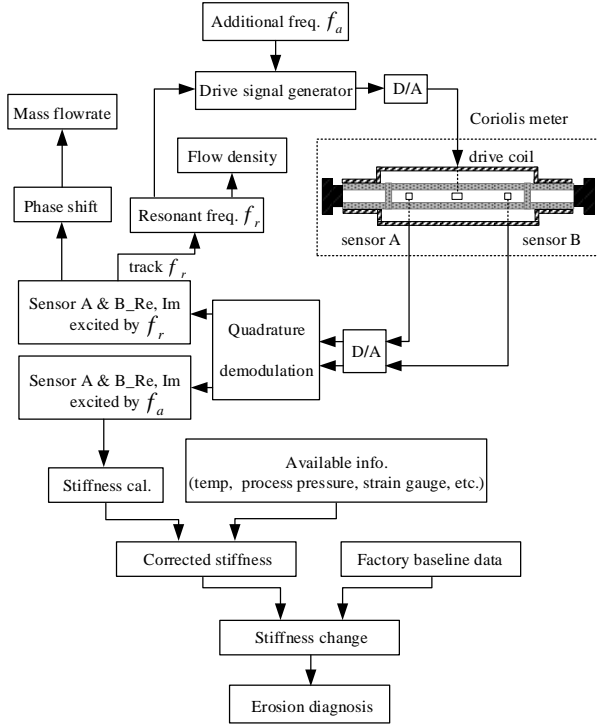


**Figure 3:** Implementation of stiffness measurement in a Coriolis flowmeter.

### 3. Simulation results and experimental validation

To validate the above theoretical analysis and evaluate the stiffness diagnostic method, analytical modelling and computational simulation were conducted using Simulink. With the aim to take the complexity of a real industrial process into account, we test various mass-spring-damper models.

#### 3.1 Simulation system

A measuring tube can be simplified by a vibration model, which is described by four key parameters, including the degrees of freedom, mass, stiffness and damping level. To investigate the effect of degrees of freedom on stiffness extraction, the simulation work begins with a simplest SDOF model. Then it is extended to a 3DOF (three-degree-of-freedom) model. Other modal parameters, namely *mass*, *stiffness* and *damping*, are set to proper values, estimated from the actual data of a commercial Coriolis flowmeter. The following calculations detail the relevant estimations, given in Equation (11). Since air is much lighter than water,  $m_{air}$  is neglected, to simplify the calculation. Likewise, we also assume that the effective vibrating mass simply equals to the mass of an empty tube plus that of the fluid.

$$\begin{cases} \omega_{r\_air} = \sqrt{\frac{k}{m_{tube}+m_{air}}} = \sqrt{\frac{k}{m_{tube}}} \\ \omega_{r\_water} = \sqrt{\frac{k}{m_{tube}+m_{water}}} = \sqrt{\frac{k}{m_{tube}+\rho_{water}A_{tube}L_{tube}}} \end{cases} \quad (11)$$

Where  $\omega_{r\_air}$  and  $\omega_{r\_water}$  represent the resonant frequencies when pure air and water flow through the tube, respectively.  $m_{tube}$  is the mass of the empty tube.  $m_{air}$  and  $m_{water}$  denote the mass of air and water inside the tube.  $m_{water}$  is determined by the water density  $\rho_{water}$  and the internal volume of the tube. With the known dimension data including the cross sectional area  $A_{tube}$  and the tube length  $L_{tube}$ ,  $m_{water}$  is estimated.

In this work, the numerical substitutions of  $\omega_{r\_air}$ ,  $\omega_{r\_water}$ ,  $A_{tube}$ , and  $L_{tube}$  are undertaken based on actual data of a DN50 Coriolis flowmeter (KROHNE OPTIMASS 6400 S50) under room temperature. Finally, the unknown stiffness  $k$  and  $m_{tube}$  are solved from Equation (11). The value of  $k$  is around  $2.4 \times 10^6$  N/m, which is used in the simulation. In terms of the low-pass filter for signal demodulation, a 16<sup>th</sup>-order Butterworth IIR filter is employed.

#### 3.2 Simulation results based on a SDOF model

A simplest SDOF model is established here. The undamped resonant frequency is assumed as 240 Hz, referred to the first working frequency of a DN50 Coriolis flowmeter mentioned above. The stiffness of the spring is supposed to be  $2.4 \times 10^6$  N/m, regarded as the reference  $k_{ref}$ . Based on the resonant frequency and stiffness values, the mass value is estimated from Equation (2), i.e. 1.0554 kg.

In order to explore the effect of damping on stiffness measurement, different damping levels are added to the model. Here the dimensionless Q factor [12] is used to characterize the damping levels in this work. Equation (12) gives the relevant calculation of Q factor. In the lightly damped case in this simulation, the Q factor is calculated to be 1592, and it is decreased to 159 in the heavily damped case.

$$Q = \frac{\omega_{r1}m_1}{c_1} \quad (12)$$

Different additional frequencies are applied into the drive signal one at a time, with frequency offset  $\Delta f = f_a - f_r = -10, -9, \dots, -3, +3, \dots, +10$  in Hz. In this way, 16 stiffness results are collected from the model, resulting from 16 different frequency locations respectively, which can imply the measurement repeatability and the influence of locations. To evaluate the stiffness diagnostic results, the absolute value of relative error (change)  $\mu_i$  is computed, corresponding to different frequency locations, through Equation (13). Then, with the aid of the 16 stiffness diagnostics, the mean value of the absolute relative error (change),  $\bar{\mu}_{ARE}$ , is calculated to evaluate the accuracy of this method, whilst the standard deviation  $\sigma_{ARE}$  is given to see the repeatability, according to Equation (14),

$$\mu_i = \left| \frac{k_{simu(i)} - k_{ref}}{k_{ref}} \right| 100\% \quad (i = 1, 2, \dots, 16) \quad (13)$$

$$\begin{cases} \bar{\mu}_{ARE} = \frac{\sum_{i=1}^{16} \mu_i}{16} \\ \sigma_{ARE} = \sqrt{\frac{\sum_{i=1}^{16} (\mu_i - \bar{\mu}_{ARE})^2}{15}} \end{cases} \quad (14)$$

Figure 4 shows the stiffness diagnostic results and the effect of different damping levels, based on a SDOF model. It can be seen that relative error (change) between the simulation results and theoretical reference values are quite small, although heavy damping levels can lead to relatively higher uncertainty. This small relative error (change) is caused by the applied Butterworth IIR filter during signal demodulation. The simulation results indicate that the stiffness diagnostic method is feasible with excellent accuracy and repeatability.

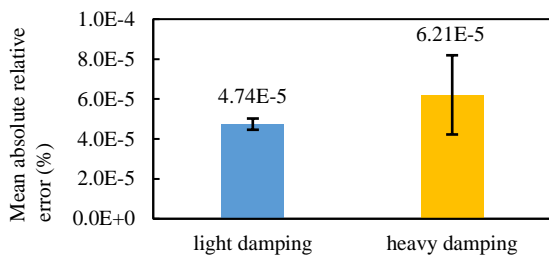


**Figure 4:** Effect of damping on stiffness measurement based on a SDOF model.

### 3.3 Simulation results based on a 3DOF model

A Coriolis oscillation system usually contains more than one degree of freedom in reality, depending on the involved specific processes. Viewing from the sensing system, we can divide a measuring tube into three concentrated elements. Among them, one element is assigned at the location of sensor A, with the lumped mass including the substitute part of empty tube part as well as the flow. Similarly, the other two elements are located near the drive coil and sensor B. Based on these substitutions, a tube can be assumed as a 3DOF system, as shown in Figure 5.

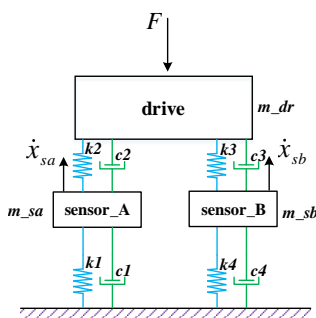


**Figure 5:** 3DOF model of the measuring tube of a Coriolis flowmeter.

The simulation system is rebuilt based on a 3DOF model. Drive signal was exerted upon the drive element, whilst

two sensor signals were picked up from sensor A and B respectively. The related modal parameters in this 3DOF model, the mass and spring stiffness, are set symmetrically with respect to the drive element. The theoretical calculations of undamped stiffness of the first oscillation mode were obtained as reference  $k_{ref\_sa}$  and  $k_{ref\_sb}$ , representing the factory baseline data. In the same way with previous work, 16 different frequencies were applied into the drive signal, with offset  $|\Delta f|$  from 3 Hz to 10 Hz, which yielded 16 pairs stiffness results,  $k_{simu\_sa(i)}$  and  $k_{simu\_sb(i)}$ , from sensor A and B, respectively.

Various damping levels were introduced in this 3DOF model to create the lightly damped and heavily damped cases. The resonant frequencies were determined by frequency sweep with an increment of 0.001 Hz. Figure 7 summarizes the stiffness diagnostic results based on a symmetric 3DOF model, which demonstrates the larger relative errors resulting from the change of damping levels. It is worth noting that, the heavy viscous damping can give rise to uncertainty in stiffness measurement, especially in a multi-degree-of-freedom (MDOF) system. The larger degrees of freedom, as well as the heavier damping levels, increase the measurement errors and uncertainties in the collected FRF data from a Coriolis sensing system, which may be affected by the adjacent vibration modes [9].

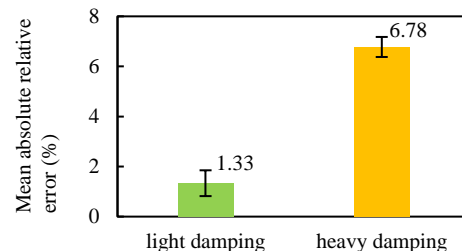


**Figure 6:** Effect of damping on stiffness measurement based on a symmetric 3DOF model.

By comparing the results in Figures 4 and 6, it can be found that, two modal parameters, the degrees of freedom and the damping levels, can affect the accuracy of stiffness measurement. Moreover, the locations of the applied additional frequencies may also cause measurement uncertainties, demonstrated by the larger standard deviation in the 3DOF case.

### 3.4 Experimental tests

With  $\pm 20$ Hz frequency offset, several tests were conducted on a DN50 Coriolis flowmeter (KROHNE OPTIMASS 6400) using tap water, under room temperature and different mass flowrates, 9t/h, 18t/h, 24t/h, 32t/h. The stiffness related diagnostic results are summarized in Figure 7. Each data point is produced

from the average values of five continuous stiffness diagnostic outputs. The maximum relative change in stiffness diagnostic results is within 0.2%, showing the good reproducibility of this method under room temperature and different mass flowrates.

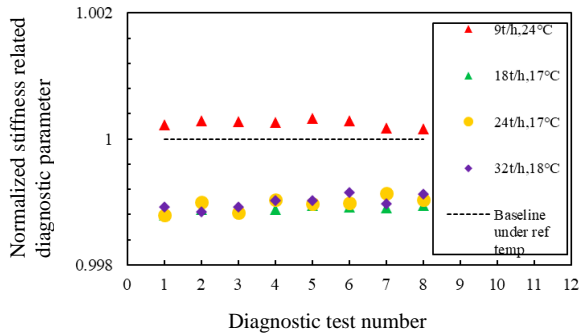


**Figure 7:** Normalized stiffness diagnostic results of a DN50 Coriolis flowmeter.

Moreover, according to the results in Figure 7, process temperature is a key factor in stiffness measurement. Temperature can not only affect the scaling constant,  $A_s$ , which is related to the drive coil and magnet units, but also influence the structural stiffness of the measuring tube. Since physical stiffness is linked to many process conditions, such as temperature, process pressure, and strain gauge [11], false alarms in stiffness diagnostics may occur when there are significant changes in process conditions.

#### 4. Conclusions

This paper provides an online in-situ method to identify the potential erosion on Coriolis flowmeters. The stiffness related diagnostic parameter is obtained to indicate the structural condition of Coriolis flowmeters, and it is proportional to the physical stiffness of the measuring tubes by a scaling factor. Based on the mathematical model of a Coriolis flowmeter, the computer simulation results have validated the feasibility of this stiffness diagnostic method. The theoretical analysis has illustrated that, two modal parameters, damping and degrees of freedom, can affect stiffness diagnostics in a Coriolis flowmeter. The larger degrees of freedom, as well as the heavier damping levels, increase the measurement errors and uncertainties in the diagnostic results, which explains the possibility of false alarms in stiffness diagnostics when the in-situ process and operation conditions deviates significantly from the factory conditions. Furthermore, experimental results obtained with a DN50 Coriolis flowmeter under room temperature have demonstrated the reproducibility of the stiffness diagnostic method with the maximum relative change in stiffness diagnostics within 0.2%.

#### References

- [1] K. J. Albion, L. Briens, C. Briens, and F. Berruti, "Multiphase flow measurement techniques for slurry transport," *Int. J. of Chem. Reac. Eng.*, vol. 9(1), 2011.
- [2] M. El-Alej, D. Mba, T. Yan, and M. Alsayh, "Identification of minimum transport condition for sand in two-phase flow using acoustic emission technology," *Appl. Acoust.* vol. 74(11), pp. 1266-1270. 2013.
- [3] Y. Faraj, M. Wang and J. Jia, "Automated Horizontal Slurry Flow Regime Recognition Using Statistical Analysis of the ERT Signal," *Procedia Engineering*, vol. 102, pp. 821-830, 2015.
- [4] G. Gao, R. Dang, A. Nouri, H. Jia, L. Li, X. Feng, and B. Dang, "Sand rate model and data processing method for non-intrusive ultrasonic sand monitoring in flow pipeline," *J. of Petro. Sci. Eng.*, vol.134, pp. 30-39, 2015.
- [5] T. Boussouara and J. P., "Assessment of erosion in flowmeters using performance and diagnostic data," 32th Int. North Sea Measurement Workshop, St Andrews, UK, Oct, 2014.
- [6] T. J. Cunningham and T. O'Banion, "Allow Smart Meter Verification to Reduce your Proving and Proof-Test Costs," 8th Int. Symposium on Fluid Flow Measurement (ISFFM), Micro Motion, 2012.
- [7] R. Baker, T. Wang, Y. Hussain and J. Woodhouse, "Method for Testing a Mass Flow Rate Meter," US 7603885B2, Oct, 2009.
- [8] E+H, flowmeters with Heartbeat Technology. Available on: <https://www.uk.endress.com/en/field-instruments-overview/product-highlights/heartbeat-technology-verification-monitoring>.
- [9] D.J. Ewins, "Modal Testing: Theory and Practice," Letchworth: Research studies press, 1984.
- [10] T. Wang and R. Baker, "Coriolis flowmeters: A review of developments over the past 20 years, and an assessment of the state of the art and likely future directions," *Flow Meas. Instrum.* vol. 40, pp. 99-123, 2014.
- [11] K. Kolahi, T. Schroder and H. Rock, "Model-based density measurement with Coriolis flowmeter," *IEEE Trans. Instrum. Meas.*, vol. 55(4), pp. 1258-1262, 2006.
- [12] J. W. Kunze, R. Storm and T. Wang, "Coriolis mass flow measurement with entrained gas," in *Proc. of Sensors and Measuring Systems*, 17th ITG/GMA Symposium, Nuremberg, Germany, Jun, 2014.
- [13] M. J. Rensing, A.T. Patten, T.J. Cunningham, and M.J. Bell, "Meter Electronics and Methods for Verification Diagnostics for a Flow Meter," US 0178738A1, Jul, 2011.